IEEE Access
Multidisciplinary | Rapid Review | Open Access Journal

Received July 4, 2017, accepted July 17, 2017, date of publication July 21, 2017, date of current version August 8, 2017.

Digital Object Identifier 10.1109/ACCESS.2017.2730223

A ULA-Based MWC Discrete Compressed Sampling Structure for Carrier Frequency and AOA Estimation

TAO CHEN, LIZHI LIU, AND DAPENG PAN

College of Information and Communication Engineering, Harbin Engineering University, Harbin, 150001, China

Corresponding author: Dapeng Pan (pandapeng@hrbeu.edu.cn)

This work was supported in part by the National Natural Science Foundation of China under Grant 61571146 and in part by the Fundamental Research Funds for the Central Universities under Grant HEUCFP201769.

ABSTRACT In this paper, we propose a new wideband digital receiver based on the modulated wideband converter (MWC) discrete compressed sampling (CS) structure, and we further propose a uniform linear array (ULA)-based MWC discrete CS structure to estimate the carrier frequency and angle-of-arrival (AOA). The proposed receiver and ULA-based system use a bank of pseudorandom sequences to mix signals to baseband and other sub-bands. The product is then low-pass filtered and down-sampled at a low rate to obtain the baseband CS data. Meanwhile, the cross-channel signal problem can be solved flexibly, since the frequency spectrum of the cross-channel signal is all mixed to the baseband. And the sensitivity can be increased a lot, because the bandwidth of the baseband is very small. However, the CS data lose the true carrier frequency and phase differences information, because of the mixing operation.Therefore, we propose to utilize the cyclic-shifted pseudorandom sequences in the ULA-based system in order to design a special phase relationship for the CS data, and on this basis, we can get the carrier frequency estimation. Then, we correct the phase differences of the CS data to estimate AOA. Finally, simulation experiments show that the proposed systems are effective and demonstrate the superior estimation performance in the case of small numbers of snapshots and low signal-to-noise ratios.

INDEX TERMS Wideband digital receiver, modulated wideband converter, compressed sampling, uniform linear array, carrier frequency and angle-of-arrival estimation.

I. INTRODUCTION

Currently wideband digital receivers are widely applied in the electronic reconnaissance to acquire signal pulse where we can get the estimations of the carrier frequency, AOA and other parameters [1]–[3]. Based on these parameters, we can identify the signal of the enemy, get technical information, and then prepare for implanting interference [4], [5]. However, with the electromagnetic environment becoming increasingly complex [6], conventional wideband digital receivers have met more and more challenges, including high sampling rates, complex structures, and cross-channel signal problems [7].

In order to solve these problems, compressed sampling theory [8]–[10] provides us a new solution to construct a brand new wideband digital receiver. In [11], an under-sampling method based on the random demodulator (RD) is proposed to decrease the sampling rate. However, the RD based system is only a sub-Nyquist sampling strategy for acquiring sparse multi-tone signals, rather than a strategy for acquiring sparse multi-band signals which are popularly utilized in the electronic reconnaissance. Reference [12] proposes a sub-Nyquist sampling method based on MWC which can realize uniform sub-Nyquist sampling for the sparse multi-band signals. Reference [13] improves MWC with run length limited sequences in the mixing operation to enlarge the input bandwidth of MWC. Reference [14] proposes a distributed MWC scheme to reduce the hardware cost. In [15], a multi-branch wideband digital reconnaissance receiver based on MWC is proposed to meet the bandwidth need of modern wideband digital receivers.

Inspired by MWC principle in continuous-time domain [12]–[15] and considering the hardware implementation, we extend MWC to discrete-time domain in order to construct a brand new wideband digital receiver. The

proposed multi-branch digital receiver can be easily realized by using FPGA development board which is skilled in parallel processing. We utilize pseudo-random sequences to mix signal to baseband and other sub-bands in each branch of the proposed receiver. Since the bandwidth of the baseband is very small, a low-rate analog-to-digital converter (ADC) can be applied in each branch to acquire baseband compressed sampling data which contain the full information of the original signal. The overall sampling rate is less than Nyquist rate, so the storage can be saved without information loss. Meanwhile, the whole design can also increase the sensitivity of the proposed receiver. Besides, cross-channel signal can be all mixed to the baseband, so we can solve the cross-channel signal problem easily just by dealing with the baseband compressed sampling data. Consequently, we can apply the proposed receiver in the electronic reconnaissance or the passive radar system to take the place of the conventional wideband digital receiver.

Moreover, it is an important task for the proposed wideband digital receiver to get the carrier frequency and AOA estimations [16]–[18]. In [19], we proposed a carrier frequency estimation method based on the proposed receiver. However, we can not get the AOA estimation with that method. Reference [20] proposes a ULA based system which adopts MWC scheme [12] to estimate carrier frequency, however, we can still not get the AOA estimation with this method. In [21], a joint spectrum sensing and direction-of-arrival (DOA) recovery method which utilizes L-shaped arrays based MWC scheme [12] is proposed, however, the estimation algorithm is complex and the system will cause a lot of operations.

In this paper, we further propose a ULA based MWC discrete compressed sampling structure where we specially adopt cyclic-shifted pseudo-random sequences in the mixing operation. Firstly, we directly process the ULA compressed sampling data instead of reconstructing original signal to reduce the complexity. Secondly, based on the theory that the shifts in time domain cause the phase shifts in frequency domain, we can get the estimation of the index of the sub-band where the carrier frequency of the original signal exists. In addition, we can estimate the carrier frequency of the baseband signal with fast Fourier transformation (FFT) frequency estimation method which is often utilized in practical application [22]. However, the true phase differences of the ULA compressed sampling data are lost because of the mixing operation. So, we propose to use a phase compensation factor to correct the phase differences. Finally, we can utilize the multiple signal classification (MUSIC) algorithm [23]–[25] to estimate AOA by processing the corrected ULA compressed sampling data. We focus on the researches how SNR and the number of snapshots influence the estimation performance. Simulations demonstrate the effectiveness of the proposed ULA based system and the proposed joint carrier frequency and AOA estimation method. Moreover, we complete an approximate carrier frequency and AOA estimation by using the proposed estimation method in the case of low SNRs and small numbers of snapshots.

The remainder of this paper is organized as follows. Section II describes the proposed new wideband digital receiver based on the MWC discrete compressed sampling structure. The ULA based MWC discrete compressed sampling structure and the joint carrier frequency and AOA estimation method are given in Section III. Finally, the simulation results and conclusions are given in Section IV and V, respectively.

II. PROPOSED MWC DISCRETE COMPRESSED SAMPLING STRUCTURE BASED RECEIVER

A. SIGNAL MODEL

The proposed receiver is designed for acquiring these signals which are popularly utilized in the electronic reconnaissance such as normal signal, binary phase shift keying (BPSK) signal, and so on. We design to detect and acquire the signal pulse in a very short time by using the proposed receiver. There would be only one signal detected and acquired in the short time. Furthermore, the probability for the electronic reconnaissance receiver to deal with multi-signals arriving simultaneously is very low [2], [3]. So, we can suppose there is only one signal received by the proposed receiver in the short sampling time. The received signal in discrete-time domain can be expressed as

$$x[n] = s[n] + \eta[n] \tag{1}$$

where $x[n]$ is the received signal, $s[n]$ is the incident signal, $\eta[n]$ is the additive complex white Gaussian noise with zero mean and σ^2 variance.

Let the received signal $x[n]$ be a complex-valued discrete-time signal with Nyquist sampling rate $f_{\mathrm{NYQ}} = 1/T_{\mathrm{NYQ}}$ and band-limited to $\mathcal{F}_{\mathrm{NYQ}} \triangleq [-f_{\mathrm{NYQ}}/2, f_{\mathrm{NYQ}}/2]$, here T_{NYQ} denotes Nyquist sampling period. So, $x[n]$ has a discrete-time Fourier transform (DTFT) and $x[n]$ can be modeled as

$$x[n] = \frac{1}{f_{\mathrm{NYQ}}} \int_{-f_{\mathrm{NYQ}}/2}^{f_{\mathrm{NYQ}}/2} X(\mathrm{e}^{j2\pi f T_{\mathrm{NYQ}}}) \mathrm{e}^{j2\pi f n T_{\mathrm{NYQ}}} df \tag{2}$$

where $X(\mathrm{e}^{j2\pi f T_{\mathrm{NYQ}}}) = \sum_{n=0}^{L_1-1} x[n] \mathrm{e}^{-j2\pi f n T_{\mathrm{NYQ}}}$, L_1 is the number of the original sampling data.

B. PRINCIPLE OF THE PROPOSED RECEIVER

As shown in Fig. 1, we propose a MWC discrete compressed sampling structure to construct a new wideband digital receiver.

The proposed receiver is comprised of M parallel branches. In the mth branch, the received signal $x[n]$ is mixed by a pseudo-random sequence $\tilde{p}_m[n]$ which is a T_p-periodic sequence with $M_p = T_p f_{\mathrm{NYQ}}$ elements per period, here T_p is the period of $\tilde{p}_m[n]$. So, $\tilde{p}_m[n]$ has a principal value sequence $p_m[n]$, depicted as

$$p_m[n] = \begin{cases} \tilde{p}_m[n], & 0 \le \mathrm{n} \le M_p - 1 \\ 0, & \text{otherwise} \end{cases} \tag{3}$$

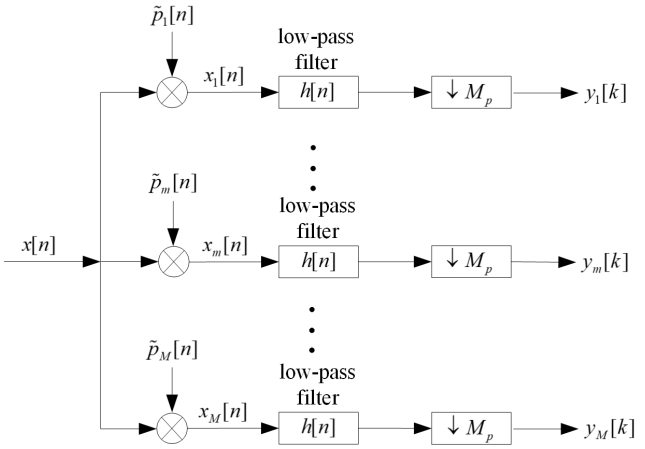

FIGURE 1. Block diagram of MWC discrete compressed sampling structure based receiver.

Furthermore, $\tilde{p}_m[n]$ has a discrete Fourier series (DFS) and $\tilde{p}_m[n]$ can be presented as

$$\tilde{p}_m[n] = \frac{1}{M_p}\sum_{l=0}^{M_p-1} P_m(l)e^{j\frac{2\pi}{M_p}nl} \tag{4}$$

where l denotes the index of the sub-band with $0 \le l \le M_p - 1$, $P_m(l)$ is digital Fourier transform coefficients of $p_m[n]$.

We define the mixing rate as $f_p = 1/T_p = f_{\mathrm{NYQ}}/M_p$ and design $f_p \ge B$ to avoid edge effects [13], here B is the bandwidth of the incident signal $s[n]$ in frequency domain. According to the spectrum distribution of the mixing function $\tilde{p}_m[n]$, we can divide the frequency band of a branch into M_p sub-bands, and the bandwidth of each sub-band is $f_p = f_{\mathrm{NYQ}}/M_p$ [12]. So, the interval of the baseband can be defined as $\mathcal{F}_p \triangleq [-f_p/2, f_p/2]$. The DTFT of the mixed signal $\tilde{x}_m[n] \triangleq x[n]\tilde{p}_m[n]$ can be evaluated as

$$\begin{aligned}
&\tilde{X}_m(e^{j2\pi fT_{\mathrm{NYQ}}}) \\
&\quad= \sum_{n=-\infty}^{\infty} x[n]\cdot\tilde{p}_m[n]e^{-j2\pi fnT_{\mathrm{NYQ}}} \\
&\quad= \sum_{n=-\infty}^{\infty} x[n]\cdot\frac{1}{M_p}\sum_{l=0}^{M_p-1} P_m(l)e^{j\frac{2\pi}{M_p}nl}e^{-j2\pi fnT_{\mathrm{NYQ}}} \\
&\quad= \frac{1}{M_p}\sum_{l=0}^{M_p-1} P_m(l)\sum_{n=-\infty}^{\infty} x[n]e^{-j(2\pi fT_{\mathrm{NYQ}}-l\frac{2\pi}{M_p})n} \\
&\quad= \frac{1}{M_p}\sum_{l=0}^{M_p-1} P_m(l)X(e^{j(2\pi fT_{\mathrm{NYQ}}-l\frac{2\pi}{M_p})}) \\
&\quad= \frac{1}{M_p}\sum_{l=0}^{M_p-1} P_m(l)X(e^{j2\pi T_{\mathrm{NYQ}}(f-lf_p)})
\end{aligned} \tag{5}$$

Then, the mixed signal $\tilde{x}_m[n]$ is low-pass filtered with a low-pass filter $h[n]$ whose frequency response $H(e^{j2\pi fT_{\mathrm{NYQ}}})$ is an ideal rectangular function in each branch. Since the baseband of the mixed signal is in the interval $\mathcal{F}_p \triangleq [-f_p/2, f_p/2]$, we design the cutoff frequency of the low-pass filter as $f_p/2$ to truncate the spectrum of the mixed signal in order to get the baseband spectrum which contain the full information of the original signal because of the mixing operation. From (5), we can see that the input of low-pass filter $H(e^{j2\pi fT_{\mathrm{NYQ}}})$ is a linear combination of f_p-shifted copies of $X(e^{j2\pi fT_{\mathrm{NYQ}}})$. So, after filtering $\tilde{x}_m[n]$ with $h[n]$, we can get the DTFT of the filtered signal $w_m[n] \triangleq \tilde{x}_m[n] * h[n]$, depicted as

$$\begin{aligned}
&W_m(e^{j2\pi fT_{\mathrm{NYQ}}}) \\
&\quad= \sum_{n=0}^{L_1-1}\tilde{x}_m[n] * h[n]e^{-j2\pi fnT_{\mathrm{NYQ}}} \\
&\quad= \tilde{X}_m(e^{j2\pi fT_{\mathrm{NYQ}}})H(e^{j2\pi fT_{\mathrm{NYQ}}}) \\
&\quad= \begin{cases} \frac{1}{M_p}\sum_{l=0}^{M_p-1} P_m(l)X(e^{j2\pi T_{\mathrm{NYQ}}(f-lf_p)}), & f\in\mathcal{F}_p \\ 0, & f\notin\mathcal{F}_p \end{cases}
\end{aligned} \tag{6}$$

where * denotes convolution operator.

According to (6), we can learn that the sampling data of the filtered signal $w_m[n]$ are redundant, because only frequencies in the baseband interval are preserved in the filtered signal $w_m[n]$ after filtering. So, we down-sample the filtered signal at a low rate $f_s = 1/T_s$ to obtain the compressed sampling data $y_m[k]$, where T_s denotes the time-interval between the compressed sampling data. For simplicity, we design $f_s = f_p = f_{\mathrm{NYQ}}/M_p$ to get the baseband interval $\mathcal{F}_p$ uniquely, where M_p is defined as the decimation factor correspondingly. We can define the compressed sampling data as $y_m[k] \triangleq \{w_m[n]\}_{\downarrow M_p}$, where $\{\cdot\}_{\downarrow M_p}$ denotes the down-sampling operation. Since the down-sampling rate of each branch is sufficiently low, existing commercial ADCs can be utilized for the down-sampling task [12]. Besides, the number of the sampling data to be processed is decreased a lot, which can contribute to reduce the computational burden, save storage space, and transmit sampling data quickly and conveniently.

Consequently, only frequencies of the filtered signal $w_m[n]$ in the interval $\mathcal{F}_s \triangleq [-f_s/2, f_s/2]$ are contained in the compressed sampling data $y_m[k]$ because of the down-sampling operation. Moreover, the compressed sampling data $y_m[k]$ turn to be band-limited to $\mathcal{F}_s$ differing from the original signal $x[n]$ which is band-limited to $\mathcal{F}_{\mathrm{NYQ}}$. Then, we can get the DTFT of the mth branch compressed sampling data $y_m[k]$, expressed as

$$\begin{aligned}
Y_m(e^{j2\pi fT_s}) &= \sum_{k=0}^{L_2-1} y_m[k]e^{-j2\pi fkT_s} \\
&= \begin{cases} \sum_{l=0}^{M_p-1} P'_m(l)X(e^{j2\pi T_{\mathrm{NYQ}}(f-lf_p)}), & f\in\mathcal{F}_s \end{cases}
\end{aligned} \tag{7}$$

where $L_2 = L_1/M_p$ is the number of the compressed sampling data in one branch, $P'_m(l) = \frac{1}{M_p}P_m(l)$.

For our purposes to consider all branches, it is convenient to write (7) in matrix form, expressed as

$$\boldsymbol{y}(f) = \boldsymbol{C}\boldsymbol{z}(f), \quad f \in \mathcal{F}_s \tag{8}$$

where $\boldsymbol{y}(f)$ is a column vector of length M with the mth element $Y_m(\mathrm{e}^{j2\pi fT_s})$, the unknown vector $\boldsymbol{z}(f) = [z_0(f), z_1(f), \cdots, z_{M_p-1}(f)]^T$ is a column vector of length M_p with $z_l(f) = X(\mathrm{e}^{j2\pi T_{\mathrm{NYQ}}(f+lf_p)}), f \in \mathcal{F}_s$. Here we use the left-shifted signal $X(\mathrm{e}^{j2\pi T_{\mathrm{NYQ}}(f+lf_p)})$ instead of the right-shifted signal $X(\mathrm{e}^{j2\pi T_{\mathrm{NYQ}}(f-lf_p)})$ of (7). Let us calculate the linear combination coefficients $P'_m(l)$

$$P'_m(l) = \frac{1}{M_p}P_m(l) = \frac{1}{M_p}\sum_{n=0}^{M_p-1} p_m[n]\mathrm{e}^{-j\frac{2\pi}{M_p}nl} \tag{9}$$

So, the compressed sampling matrix $\boldsymbol{C}$ of size $M \times M_p$ can be expressed as

$$\boldsymbol{C} = \frac{1}{M_p}\boldsymbol{P}\boldsymbol{F} \tag{10}$$

where $\boldsymbol{P}$ denotes $M \times M_p$ pseudo-random sequence matrix with $p_{m,l} \in \{+1, -1\}$, $\boldsymbol{F}$ denotes $M_p \times M_p$ discrete Fourier transform matrix with the column vector $\boldsymbol{F}_l = [1, \mathrm{e}^{j2\pi l/M_p}, \cdots, \mathrm{e}^{j2\pi(M_p-1)l/M_p}]^T$ where $(\cdot)^T$ denotes the transpose.

We can further expand (8) as

$$\underbrace{\begin{pmatrix} Y_1(\mathrm{e}^{j2\pi fT_s}) \\ Y_2(\mathrm{e}^{j2\pi fT_s}) \\ \vdots \\ Y_M(\mathrm{e}^{j2\pi fT_s}) \end{pmatrix}}_{y(f)} = \frac{1}{M_p}\underbrace{\begin{bmatrix} p_{1,0} & \cdots & p_{1,M_p-1} \\ \vdots & \ddots & \vdots \\ p_{M,0} & \cdots & p_{M,M_p-1} \end{bmatrix}}_{P}$$
$$\cdot \underbrace{\begin{bmatrix} | & \cdots & | & \cdots & | \\ F_0 & \cdots & F_l & \cdots & F_{M_p-1} \\ | & \cdots & | & \cdots & | \end{bmatrix}}_{F}$$
$$\times \underbrace{\begin{bmatrix} X(\mathrm{e}^{j2\pi T_{\mathrm{NYQ}}f}) \\ \vdots \\ X(\mathrm{e}^{j2\pi T_{\mathrm{NYQ}}(f+l\cdot f_p)}) \\ \vdots \\ X(\mathrm{e}^{j2\pi T_{\mathrm{NYQ}}(f+(M_p-1)\cdot f_p)}) \end{bmatrix}}_{z(f)} \tag{11}$$

Here we take an example to further describe the theory and advantage of the proposed receiver. Assume that $x[n]$ is a multi-band signal with spectrally sparse level $K_{sp} = 2$. We show the frequency spectrum of $x[n]$, which are depicted as a rectangle band and a triangle band in Fig. 2. Meanwhile, we give the Fourier transform coefficients of $p_m[n]$, which are equidistant discrete spectral lines plotted in red lines in Fig. 2.

According to (5), $\tilde{X}_m(\mathrm{e}^{j2\pi fT_{\mathrm{NYQ}}})$ which is shown in Fig. 3 is a linear combination of f_p-shifted copies of $\tilde{X}(\mathrm{e}^{j2\pi fT_{\mathrm{NYQ}}})$. From Fig. 3, we know the frequency spectrum of the mixed signal $\tilde{x}_m[n]$ is divided into many different sub-band spectrums. All information of $x[n]$ is contained in each sub-band and only the weighted coefficients of linear combination are different, i.e., mixing operation folds frequency spectrum to sub-bands with different weights for each frequency interval, which is the reason why we can solve the cross-channel signal problem easily. Only baseband signal which is shown in solid line box in Fig. 3 is low-pass filtered and then down-sampled to obtain the compressed sampling data, which is the reason why the sensitivity of the proposed receiver increases.

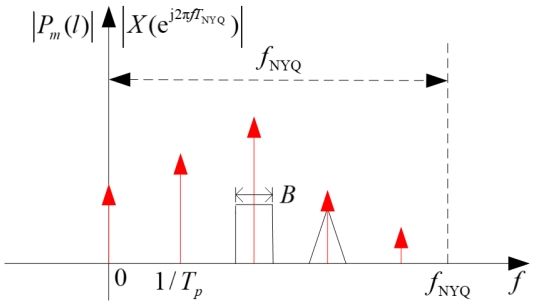

FIGURE 2. Frequency spectrum of a multiband signal and a mixing function.

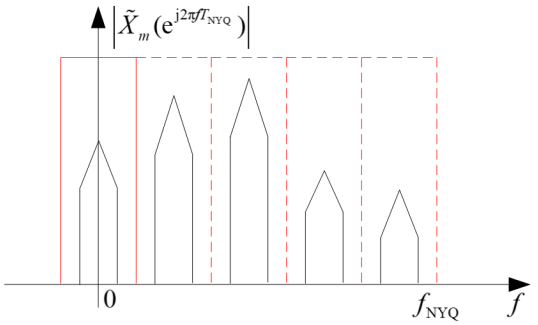

FIGURE 3. Frequency spectrum of the mixing signal.

III. PROPOSED ULA BASED SYSTEM FOR CARRIER FREQUENCY AND AOA ESTIMATION

A. ARRAY SIGNAL MODEL

We propose a ULA based MWC discrete compressed sampling structure to estimate the carrier frequency and AOA simultaneously instead of the proposed receiver applied in the electronic reconnaissance. So, we still suppose only one far-field discrete-time signal impinging on the ULA based system which has M antenna array elements spacing d from direction θ which should be limited to the scope of AOA estimation for the ULA, i.e., $\theta \in (-90°, 90°)$ [20]. The received signal in spatial domain can be expressed as

$$\boldsymbol{x}[n] = \boldsymbol{A}s[n] + \boldsymbol{\eta}[n], \quad n = 1, 2, \cdots, L_1 \tag{12}$$

where $\boldsymbol{x}[n] = [x_1[n], x_2[n], \cdots, x_M[n]]^T$ is the $M \times 1$ received signal vector, $\boldsymbol{A} = [\boldsymbol{a}(\theta)]$ is the array manifold matrix, $\boldsymbol{a}(\theta) = [1, \mathrm{e}^{-j\frac{2\pi d}{\lambda}\sin\theta}, \cdots, \mathrm{e}^{-j\frac{2\pi(M-1)d}{\lambda}sin\theta}]^T$ is the steering vector of the array, λ is the carrier wavelength,

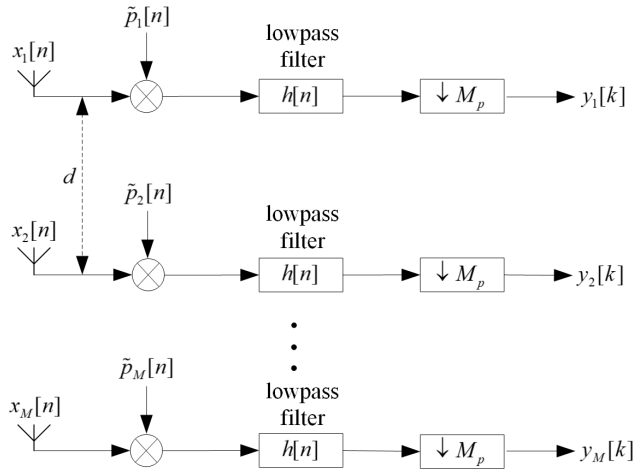

FIGURE 4. Block diagram of ULA based MWC discrete compressed sampling structure.

$s[n]$ is the incident signal, $\boldsymbol{\eta}[n] = [\eta_1[n], \eta_2[n], \cdots, \eta_M[n]]^T$ is $M \times 1$ additive complex white Gaussian noise vector with zero mean and σ^2 variance, L_1 is the original number of snapshots correspondingly.

Let the incident $s[n]$ be a complex-valued discrete-time signal with Nyquist sampling rate f_{NYQ} and band-limited to $\mathcal{F}_{\mathrm{NYQ}} \triangleq [-f_{\mathrm{NYQ}}/2, f_{\mathrm{NYQ}}/2]$. So, $s[n]$ has a DTFT and $s[n]$ can be expressed as

$$s[n] = \frac{1}{f_{\mathrm{NYQ}}} \int_{-f_{\mathrm{NYQ}}/2}^{f_{\mathrm{NYQ}}/2} S(\mathrm{e}^{j2\pi f T_{\mathrm{NYQ}}}) \mathrm{e}^{j2\pi f n T_{\mathrm{NYQ}}} df \tag{13}$$

where $S(\mathrm{e}^{j2\pi f T_{\mathrm{NYQ}}}) = \sum_{n=0}^{L_1-1} s[n] \mathrm{e}^{-j2\pi f n T_{\mathrm{NYQ}}}$.

B. PRINCIPLE OF THE ULA BASED SYSTEM

In this section, a ULA based MWC discrete compressed sampling structure is proposed to carry out carrier frequency and AOA estimation simultaneously as shown in Fig. 4. It should be noticed that the structure of the proposed receiver is very suitable to process the array signals because of the parallel multi-branch structure. We implement an antenna in each branch of the proposed receiver to build a ULA based system. In each branch of the ULA based system, the received signal is mixed by the cyclic-shifted pseudo-random sequence, low-pass filtered and down-sampled at a low rate to obtain compressed sampling data. So, the proposed ULA based system also has these advantages such as realizing sub-Nyquist sampling, solving the cross-channel signal problem flexibly, and having a low complexity of hardware implementation.

We utilize the cyclic-shifted pseudo-random sequence $\tilde{p}_m[n]$ $(1 \le m \le M)$ with the mixing rate $f_p = 1/T_p = f_{\mathrm{NYQ}}/M_p$ to mix the received signal $x_m[n]$ orderly in each branch. Assume that the principal value sequence $p_m[n]$ of the cyclic-shifted pseudo-random sequence $\tilde{p}_m[n]$ is the cyclic shifts of the principal value sequence $p_1[n]$ of the cyclic-shifted pseudo-random sequence $\tilde{p}_1[n]$, expressed as

$$p_m[n] = p_1[n - m + 1] \tag{14}$$

So, $\tilde{p}_m[n]$ has a DFS and $\tilde{p}_m[n]$ can be expressed as

$$\begin{aligned} \tilde{p}_m[n] &= \frac{1}{M_p} \sum_{l=0}^{M_p-1} P_m(l) \mathrm{e}^{j\frac{2\pi}{M_p} nl} \\ &= \frac{1}{M_p} \sum_{l=0}^{M_p-1} P_1(l) \mathrm{e}^{j\frac{2\pi}{M_p}(n-m+1)l} \end{aligned} \tag{15}$$

According to (5), the DTFT of the mixed signal $\tilde{s}_m[n] \triangleq s[n]\tilde{p}_m[n]$ in the mth branch can be evaluated as

$$\begin{aligned} &\tilde{S}_m(\mathrm{e}^{j2\pi f T_{\mathrm{NYQ}}}) \\ &\quad = \frac{1}{M_p} \sum_{l=0}^{M_p-1} P_1(l) S(\mathrm{e}^{j2\pi T_{\mathrm{NYQ}}(f - l f_p)}) \mathrm{e}^{-j\frac{2\pi}{M_p}(m-1)l} \end{aligned} \tag{16}$$

After mixing, the spectrum of the mixed signal is truncated to obtain the baseband interval $\mathcal{F}_p \triangleq [-f_p/2, f_p/2]$ by a low-pass filter with the cutoff frequency $f_p/2$ and the filtered signal is down-sampled at a low rate $f_s = f_p = f_{\mathrm{NYQ}}/M_p$ to obtain the compressed sampling data. So, the DTFT of the compressed sampling data $\bar{s}_m[k] \triangleq \{\tilde{s}_m[n] * h[n]\}_{\downarrow M_p}$ can be expressed as

$$\begin{aligned} &\bar{S}_m(\mathrm{e}^{j2\pi f T_s}) \\ &\quad = \sum_{k=0}^{L_2-1} \bar{s}_m[k] \mathrm{e}^{-j2\pi f k T_s} \\ &\quad = \frac{1}{M_p} \sum_{l=0}^{M_p-1} P_1(l) S(\mathrm{e}^{j2\pi T_{\mathrm{NYQ}}(f - l f_p)}) \mathrm{e}^{-j\frac{2\pi}{M_p}(m-1)l}, \quad f \in \mathcal{F}_s \end{aligned} \tag{17}$$

where $\bar{s}_m[k]$ is the compressed sampling data of the incident signal $s[n]$ in the mth branch of the ULA based system, $L_2 = L_1/M_p$ is the number of the snapshots after compressed sampling correspondingly.

So, the mth branch output of the ULA based system in spatial domain can be expressed as

$$\begin{aligned} &y_m[k] \\ &= \{(x_m[n] \cdot \tilde{p}_m[n]) * h[n]\}_{\downarrow M_p} \\ &= \left\{(\mathrm{e}^{-j2\pi d \sin(\theta)/\lambda})^{m-1} ((s[n] \cdot \tilde{p}_m[n]) * h[n])\right\}_{\downarrow M_p} \\ &\quad + \{(\eta_m[n] \cdot \tilde{p}_m[n]) * h[n]\}_{\downarrow M_p} \\ &= \left\{(\mathrm{e}^{-j2\pi d \sin(\theta)/\lambda})^{m-1} (\frac{1}{M_p} \sum_{l=0}^{M_p-1} P_1(l) \mathrm{e}^{j\frac{2\pi}{M_p}(n-m+1)l}) s[n]\right\}_{\downarrow M_p} \\ &\quad + \bar{\eta}_m[k] \end{aligned} \tag{18}$$

where $y_m[k]$ is compressed sampling data of the received signal $x_m[n]$ in the mth branch of the ULA based system, $\bar{\eta}_m[k]$ is the compressed sampling data of the original additive complex white Gaussian noise $\eta_m[k]$ in the mth branch of

the ULA based system and $\bar{\eta}_m[k]$ becomes the uncorrelated band-limited additive complex white noise with zero mean and σ^2/M_p variance.

Since the sub-band bandwidth f_p is designed larger than the incident signal bandwidth B, depicted as $f_p \geq B$. So, we know that the carrier frequency of the incident signal $s[n]$ only exists in an unknown l'th ($0 \leq l' \leq M_p - 1$) sub-band in each branch of the ULA based system. Then, the spectrum information of other sub-bands in each branch can be approximately ignored since there are very little spectrum information of the incident signal in those sub-bands except the $l'th$ sub-band. Thus, (18) can be also written as

$$y_m[k] \approx \left\{ (\mathrm{e}^{-j2\pi d \sin(\theta)/\lambda} \mathrm{e}^{-j\frac{2\pi}{M_p}l'})^{m-1} \frac{1}{M_p} P_1(l') \mathrm{e}^{j\frac{2\pi}{M_p}nl'} s[n] \right\}_{\downarrow M_p} + \bar{\eta}_m[k] \quad (19)$$

Considering (19), we can learn that the mixing operations make the compressed sampling data lose the true carrier frequency and phase differences. So, we can not get the carrier frequency and AOA estimation only by directly processing the compressed sampling data. In order to get the AOA estimation, we have to remove the factor $\exp(-j2\pi(m-1)l'/M_p)$ from (19) to correct phase differences of the compressed sampling data. So, let us discuss how to estimate the sub-band index l' and the carrier frequency f_c firstly.

C. CARRIER FREQUENCY ESTIMATION

We randomly choose two branches of the ULA based system depicted as the mth branch and $(m+1)$th branch to describe the carrier frequency estimation method. According to (19), we can get the DTFTs of the compressed sampling data of the received signal $x_m[n]$ in the mth branch and $(m+1)$th branch of the ULA based system, respectively expressed as

$$\begin{aligned} &Y_m(\mathrm{e}^{j2\pi fT_s}) \\ &\quad \approx (\mathrm{e}^{-j2\pi d \sin(\theta)/\lambda})^{m-1} \frac{1}{M_p} P_1(l') \\ &\qquad \cdot X(\mathrm{e}^{j2\pi T_{\mathrm{NYQ}}(f-l'f_p)}) \mathrm{e}^{-j\frac{2\pi}{M_p}(m-1)l'}, \quad f \in \mathcal{F}_s \end{aligned} \quad (20)$$

$$\begin{aligned} &Y_{m+1}(\mathrm{e}^{j2\pi fT_s}) \\ &\quad \approx (\mathrm{e}^{-j2\pi d \sin(\theta)/\lambda})^{m} \frac{1}{M_p} P_1(l') \\ &\qquad \cdot X(\mathrm{e}^{j2\pi T_{\mathrm{NYQ}}(f-l'f_p)}) \mathrm{e}^{-j\frac{2\pi}{M_p}ml'}, \quad f \in \mathcal{F}_s \end{aligned} \quad (21)$$

Then, the ratio of $Y_{m+1}(\mathrm{e}^{j2\pi fT_s})$ to $Y_m(\mathrm{e}^{j2\pi fT_s})$ can be expressed as

$$\begin{aligned} &\frac{Y_{m+1}(\mathrm{e}^{j2\pi fT_s})}{Y_m(\mathrm{e}^{j2\pi fT_s})} \\ &\approx \frac{(\mathrm{e}^{-j2\pi d \sin(\theta)/\lambda})^{m} \frac{1}{M_p} P_1(l') X(\mathrm{e}^{j2\pi T_{\mathrm{NYQ}}(f-l'f_p)}) \mathrm{e}^{-j\frac{2\pi}{M_p}ml'}}{(\mathrm{e}^{-j2\pi d \sin(\theta)/\lambda})^{m-1} \frac{1}{M_p} P_1(l') X(\mathrm{e}^{j2\pi T_{\mathrm{NYQ}}(f-l'f_p)}) \mathrm{e}^{-j\frac{2\pi}{M_p}(m-1)l'}} \\ &\approx \mathrm{e}^{-j2\pi d \sin(\theta)/\lambda} \mathrm{e}^{-j\frac{2\pi}{M_p}l'} \\ &\approx \mathrm{e}^{-j2\pi f \Delta\tau} \mathrm{e}^{-j\frac{2\pi}{M_p}l'}, \quad f \in \mathcal{F}_s \end{aligned} \quad (22)$$

where the difference $\Delta\tau = \tau_{m+1} - \tau_m = d\sin(\theta)/c$, $\tau_m = (m-1)d\sin(\theta)/c$ is the time delay at the mth antenna with respect to the first antenna and c is the speed of light.

In order to get the estimation of the sub-band index l', we should remove the factor $\exp(-j2\pi f\Delta\tau)$ from the ratio $Y_{m+1}(\mathrm{e}^{j2\pi fT_s})/Y_m(\mathrm{e}^{j2\pi fT_s})$ shown in (22). We know the difference of the time delay $\Delta\tau$ can cause $\Delta\tau \cdot f_{\mathrm{NYQ}}$ sampling points delay in discrete-time domain. So, we can delay the mth branch compressed sampling data k_d points to produce a phase compensation for the ratio in (22), expressed as

$$\mathrm{DTFT}\{y_m[k-k_d]\} = \mathrm{e}^{-j2\pi fT_s k_d} Y_m(\mathrm{e}^{j2\pi fT_s}), \quad f \in \mathcal{F}_s \quad (23)$$

Then, we make

$$2\pi fT_s k_d = 2\pi fT_{\mathrm{NYQ}} \Delta\tau \times f_{\mathrm{NYQ}} \quad (24)$$

Simplify (24), we have

$$k_d = \frac{T_{\mathrm{NYQ}}}{T_s} \Delta\tau \times f_{\mathrm{NYQ}} = \Delta\tau \times \frac{f_{\mathrm{NYQ}}}{M_p} = \Delta\tau \times f_s \quad (25)$$

Since we know the value of M_p and the value of f_{NYQ}. In addition, the difference of the time delay $\Delta\tau = \tau_{m+1} - \tau_m = d\sin(\theta)/c = \tau_2$ can be estimated by calculating the time delay at the second antenna with respect to the first antenna [26]. So, after the delaying operation, we can further rewrite (22) as

$$\frac{\widehat{Y}_{m+1}(\mathrm{e}^{j2\pi fT_s})}{\widehat{Y}_m(\mathrm{e}^{j2\pi fT_s})} = \mathrm{e}^{-j\frac{2\pi}{M_p}l'}, \quad f \in \mathcal{F}_s \quad (26)$$

where we define $\widehat{Y}_m(\mathrm{e}^{j2\pi fT_s}) \triangleq \sum_{k=k_d}^{L_2-1} y_m[k]\mathrm{e}^{-j2\pi fkT_s}$ and define $\widehat{Y}_{m+1}(\mathrm{e}^{j2\pi fT_s}) \triangleq \sum_{k=0}^{L_2-k_d-1} y_{m+1}[k]\mathrm{e}^{-j2\pi fkT_s}$ correspondingly.

Thus, we can get the estimation of the sub-band index l' according to (26), depicted as

$$l' = \frac{M_p}{2\pi} \left| \ln\left(\frac{\widehat{Y}_{m+1}(\mathrm{e}^{j2\pi fT_s})}{\widehat{Y}_m(\mathrm{e}^{j2\pi fT_s})}\right) \right|, \quad f \in \mathcal{F}_s \quad (27)$$

Finally, the carrier frequency estimation of the incident signal $s[n]$ can be expressed as

$$f_c' = l' \times f_p + \Delta f \quad (28)$$

where f_p denotes the bandwidth of a sub-band, f_c' is the estimation of the original carrier frequency f_c, and Δf is the carrier frequency estimation of the baseband signal which can be obtained with the FFT frequency estimation method [22].

In order to get better carrier frequency estimation performance and fully utilize the multi-branch structure, we can utilize all branches of compressed sampling data to get a set of l' estimations. Then, we choose the mode from them as the final l' estimation. Since the carrier frequencies of baseband signal in each branch are all the same, we only need to process any branch of compressed sampling data to get Δf estimation. Finally, we can get a more accurate carrier frequency estimation f_c'.

D. AOA ESTIMATION

We can expand (18) as

$$\begin{bmatrix} y_1[k] \\ y_2[k] \\ \vdots \\ y_M[k] \end{bmatrix} = \begin{bmatrix} 1 \cdot \bar{s}_1[k] \\ e^{-j\frac{2\pi d}{\lambda}\sin\theta} \cdot \bar{s}_2[k] \\ \vdots \\ e^{-j\frac{2\pi(M-1)d}{\lambda}\sin\theta} \cdot \bar{s}_M[k] \end{bmatrix} + \begin{bmatrix} \bar{\eta}_1[k] \\ \bar{\eta}_2[k] \\ \vdots \\ \bar{\eta}_M[k] \end{bmatrix} \quad (29)$$

In order to correct the phase differences of the compressed sampling data, we propose to utilize a correction factor $\exp(j\frac{2\pi}{M_p}(m-1)l')$ to multiply the mth branch compressed sampling data $y_m[k]$ according to (19). Then, we have

$$\begin{aligned} \begin{bmatrix} \hat{y}_1[k] \\ \hat{y}_2[k] \\ \vdots \\ \hat{y}_M[k] \end{bmatrix} &= \begin{bmatrix} 1 \cdot y_1[k] \\ e^{j\frac{2\pi}{M_p}l'} \cdot y_2[k] \\ \vdots \\ e^{j\frac{2\pi}{M_p}(M-1)l'} \cdot y_M[k] \end{bmatrix} \\ &= \begin{bmatrix} 1 \cdot 1 \cdot \bar{s}_1[k] \\ e^{j\frac{2\pi}{M_p}l'} \cdot e^{-j\frac{2\pi d}{\lambda}\sin\theta} \cdot \bar{s}_2[k] \\ \vdots \\ e^{j\frac{2\pi}{M_p}(M-1)l'} \cdot e^{-j\frac{2\pi(M-1)d}{\lambda}\sin\theta} \cdot \bar{s}_M[k] \end{bmatrix} \\ &\quad + \begin{bmatrix} 1 \cdot \bar{\eta}_1[k] \\ e^{j\frac{2\pi}{M_p}l'} \cdot \bar{\eta}_2[k] \\ \vdots \\ e^{j\frac{2\pi}{M_p}(M-1)l'} \cdot \bar{\eta}_M[k] \end{bmatrix} \\ &\triangleq \begin{bmatrix} 1 \\ e^{-j\frac{2\pi d}{\lambda}\sin\theta} \\ \vdots \\ e^{-j\frac{2\pi(M-1)d}{\lambda}\sin\theta} \end{bmatrix} \hat{s}[k] + \begin{bmatrix} \hat{\eta}_1[k] \\ \hat{\eta}_2[k] \\ \vdots \\ \hat{\eta}_M[k] \end{bmatrix} \end{aligned} \quad (30)$$

where $\hat{s}[k] = \exp(j\frac{2\pi}{M_p}(m-1)l') \cdot \bar{s}_m[k]$ is the corrected compressed sampling data of the incident signal and $\hat{\eta}[k] = \exp(j2\pi(m-1)l'/M_p) \cdot \bar{\eta}_m[k]$ is the corrected uncorrelated band-limited additive complex white noise with zero mean and σ^2/M_p variance in mth branch.

We can further write Equation (30) in matrix form

$$\hat{y}[k] = \boldsymbol{A}\hat{s}[k] + \hat{\eta}[k], \quad k = 1, 2, \cdots, L_2 \quad (31)$$

where $\hat{y}[k] = [\hat{y}_1[k], \hat{y}_2[k], \cdots, \hat{y}_M[k]]^T$ is $M \times 1$ corrected compressed sampling outputs vector, $\hat{\eta}[k] = [\hat{\eta}_1[k], \hat{\eta}_2[k], \cdots, \hat{\eta}_M[k]]^T$ is $M \times 1$ corrected uncorrelated band-limited additive complex white noise vector.

As we have assumed that we can only get one source in a short sampling time with the ULA based system, we can utilize the high-resolution MUSIC algorithm [23]–[25] to process the compressed sampling data $\hat{\boldsymbol{y}}[k]$ in order to get the AOA estimation. The array covariance matrix is

$$\boldsymbol{R}_{\hat{y}} = E\{\hat{\boldsymbol{y}}\hat{\boldsymbol{y}}^{\mathrm{H}}\} = \boldsymbol{A}\boldsymbol{R}_{\hat{s}}\boldsymbol{A} + \frac{\sigma^2}{M_p}\boldsymbol{I}_M \quad (32)$$

where $(\cdot)^{\mathrm{H}}$ denotes the conjugate transpose, $E\{\cdot\}$ denotes the expectation, $\boldsymbol{R}_{\hat{s}} = E\{\hat{s}\hat{s}^{\mathrm{H}}\}$ is the covariance matrix of the corrected compressed sampling data of the incident signal, $\boldsymbol{I}_M$ denotes an identity matrix of size $M \times M$.

As the number of snapshots is finite in practice, the practical sampling covariance matrix is given by

$$\boldsymbol{R}_{\hat{y}} = \frac{1}{L_2}\sum_{k=0}^{L_2-1} \hat{\boldsymbol{y}}[k]\hat{\boldsymbol{y}}^{\mathrm{H}}[k] \quad (33)$$

After eigenvalue decomposition for $\boldsymbol{R}_{\hat{y}}$, we can get MUSIC spectrum, expressed as

$$P_{\mathrm{MUSIC}}(\theta) = \frac{1}{a^{\mathrm{H}}(\theta)U_{\mathrm{N}}U_{\mathrm{N}}^{\mathrm{H}}a(\theta)} \quad (34)$$

where $\boldsymbol{U}_{\mathrm{N}}$ denotes the noise sub-space.

Finally, we can get the AOA estimation through searching the peak of the MUSIC spectrum $P_{\mathrm{MUSIC}}(\theta)$. The estimated AOA can be expressed as

$$\theta = \arg_\theta \min \boldsymbol{a}^{\mathrm{H}}(\theta)\boldsymbol{U}_{\mathrm{N}}\boldsymbol{U}_{\mathrm{N}}^{\mathrm{H}}\boldsymbol{a}(\theta) \quad (35)$$

IV. SIMULATION EXPERIMENTS

We conducted computer simulations with MATLAB R2016a to validate the carrier frequency and AOA estimation performance of the proposed ULA based system. The simulations use root mean square error (RMSE) to analyze the carrier frequency and AOA estimation performance, expressed as

$$\mathrm{RMSE} = \sqrt{\frac{1}{J}\sum_{j=1}^{J}(\alpha_j' - \alpha)^2} \quad (36)$$

where J is the times of independent Monte Carlo simulations, α_j' denotes the carrier frequency or AOA estimation value of the true carrier frequency or AOA depicted as α for the jth trial.

A. CARRIER FREQUENCY ESTIMATION PERFORMANCE

In this section, we consider a ULA based system with ten antennas, in which the distance between adjacent elements is half-wavelength [27]. The cyclic-shifted pseudo-random sequence is completed by Bernoulli random binary ± 1 sequence with $M_p = 100$, so the bandwidth of the baseband is $f_p = f_{\mathrm{NYQ}}/M_p = 22$ MHz. Here ideal low-pass filter with cutoff frequency $f_p/2$ is used and the down-sampling rate $f_s = f_p = 22$ MHz is designed. Assume that a normal signal with Nyquist sampling rate $f_{\mathrm{NYQ}} = 2.2$ GHz, $f_c = 1$ GHz and $\theta = 5°$ impinges on the ULA based system.

As we know, MWC [12] and RD [11] are the two of the most popular sub-Nyquist sampling structures. In order to validate the effectiveness of the proposed receiver and ULA based system, we carry out the same simulations with RD structure whose module parameters are designed as the same as the corresponding modules in one branch of the ULA based system as comparisons.

Fig. 5(a) and Fig. 5(b) show the frequency spectrums of the RD compressed sampling data and the three branches of

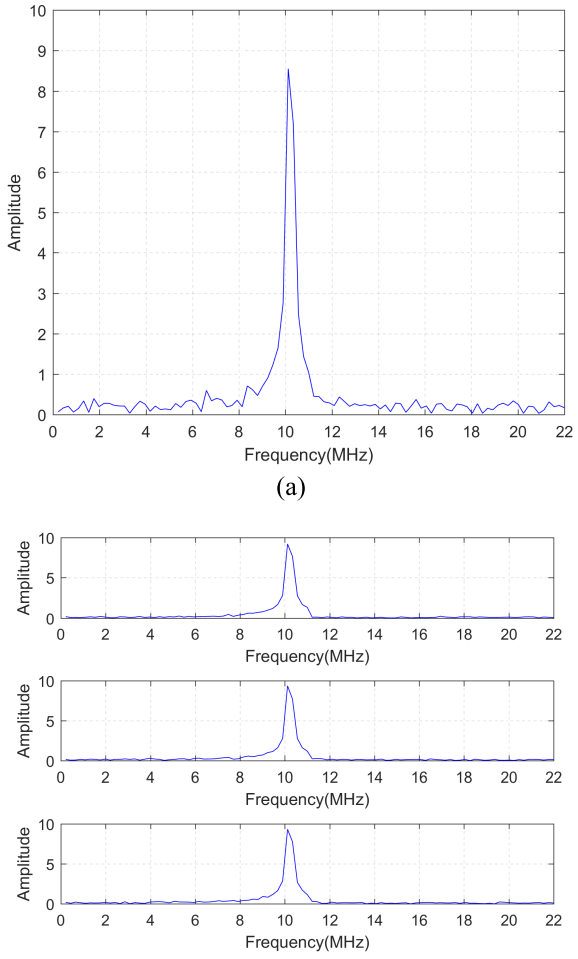

FIGURE 5. Frequency spectrum of the baseband compressed sampling data with SNR = 15 dB. (a) RD, (b) three branches of the ULA based system.

compressed sampling data which are randomly selected from the ULA based system with SNR = 15 dB, respectively. By comparison, we can see that the baseband compressed sampling data of the two different systems can keep the full frequency information of the incident normal signal. However, we can not get the index of the number of the sub-band where the incident signal exists just by processing only one branch of the compressed sampling data without reconstruction. Besides, we can not get the array signal model to estimate AOA due to the one-branch sub-Nyquist sampling structure. We can solve these problems with the proposed receiver and ULA system which utilize the multi-branch MWC discrete compressed sampling structure.

Then, we analyze the original carrier frequency estimation performance versus SNR with the number of snapshots $L_2 = 100$. The SNR varies from -10 dB to 20 dB with 5 dB steps. Monte Carlo experiments will be done 100 times in each SNR to count the RMSE of carrier frequency estimation. We set up $f_c = 1$ GHz fixedly in each trial to get the RMSE

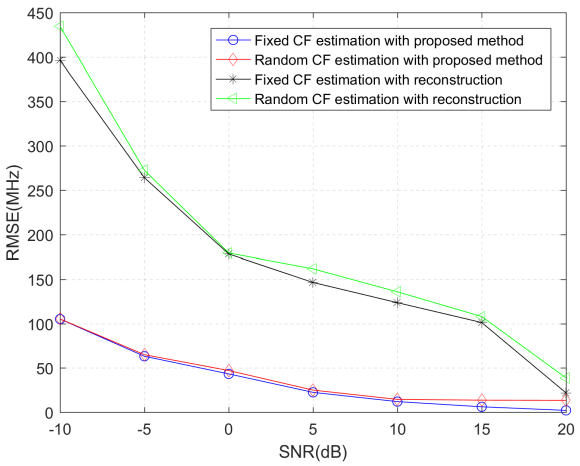

FIGURE 6. RMSE of the carrier frequency estimation versus SNR.

of the original carrier frequency estimation. And in order to validate the robustness of the proposed carrier frequency estimation method, we randomly choose f_c from the range [1000 MHz, 1050 MHz] in each trial for another RMSE of the original carrier frequency estimation. Besides, in order to prove that the computational complexity will decrease by directly processing the compressed sampling data, we carry out the same simulations by processing the reconstructed signal in the ULA based system, where the continuous-to-finite (CTF) and orthogonal matching pursuit (OMP) algorithms are used to reconstruct the original signal [12] and the FFT method are used to estimate the original carrier frequency. As shown in Table I, the proposed ULA based system spends about 1 s to get the compressed sampling data and about 1.6 s to get the reconstructed signal for one hundred trials, respectively. So, we can save a considerable amount of time to get the data to be processed without reconstruction. The variety of SNR has little effect on the computational complexity of the proposed system. The RMSEs of the four simulations versus SNR are shown in Fig. 6, where CF denotes the carrier frequency. We can learn from Fig. 6 that the RMSEs of the four simulations decrease with the increase of the SNR. Moreover, the RMSE of the proposed method is far less than the RMSE of the carrier frequency estimation of the reconstructed signal in the case of $-10\text{ dB} \leq \text{SNR} < 20$ dB, which validate the effectiveness of the proposed carrier frequency estimation method.

TABLE 1. Computational complexity test (unit: s).

SNR	ULA based system without reconstruction	ULA based system with reconstruction
-10 dB	1.014	1.679
0 dB	1.006	1.665
20 dB	0.980	1.647

Then, we discuss how the estimation of the sub-band index l' and the estimation of baseband carrier frequency Δf influence the original carrier frequency estimation

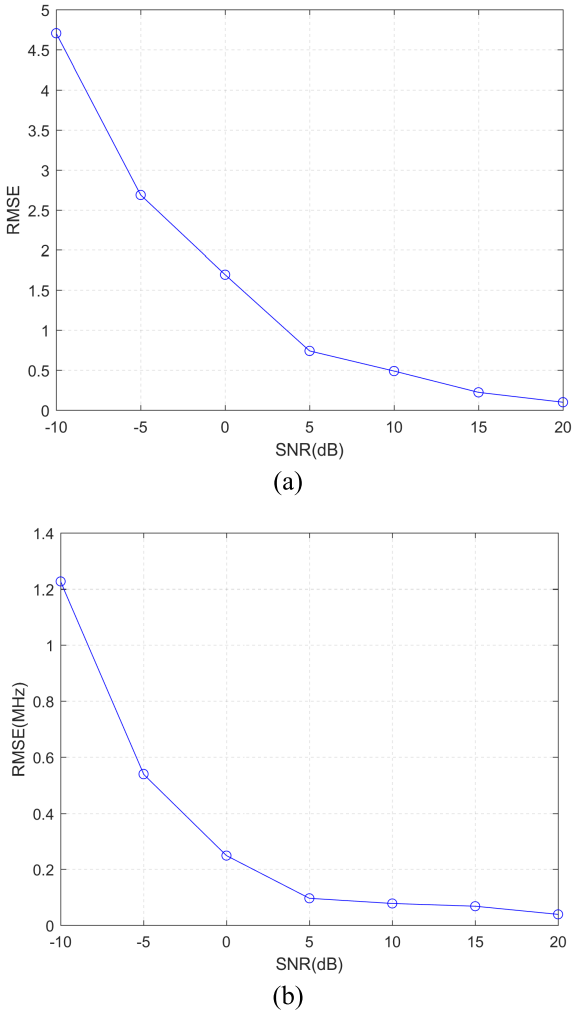

FIGURE 7. RMSE. (a) RMSE of the sub-band index l' estimation versus SNR. (b) RMSE of baseband carrier frequency estimation versus SNR.

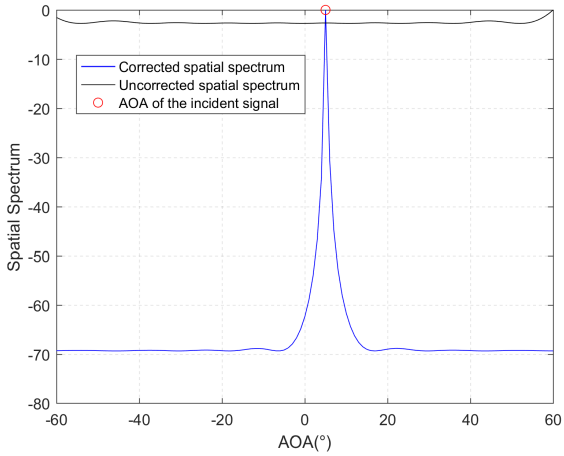

FIGURE 8. The spatial spectrum of the compressed sampling data.

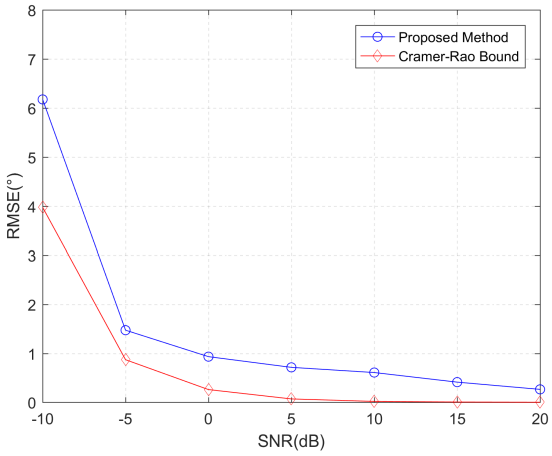

FIGURE 9. RMSE of AOA estimation versus SNR.

performance when the original carrier frequency is set up $f_c = 1$ GHz. Fig. 7(a) shows the RMSE of l' estimation versus SNR. We can learn from Fig. 7(a) that the RMSE of l' estimation decreases with the increase of the SNR. However, when SNR ≤ 0 dB, the RMSE of l' estimation will be more than 1.5, which will generate large RMSEs for the original carrier frequency estimation because of the large bandwidth of the sub-band ($f_p = 22$ MHz). The RMSE of the baseband carrier frequency estimation Δf versus SNR is shown in Fig. 7(b). It can be seen from Fig. 7(b) that the baseband carrier frequency estimation Δf have little effect on the original carrier frequency estimation f_c'.

B. AOA ESTIMATION PERFORMANCE

In this section, we analyze the AOA estimation performance versus SNR, as well as the AOA estimation performance versus number of snapshots. The simulation parameters are set as the same as the simulation above. Monte Carlo experiments will be done 100 times for each SNR or number of snapshots to count the RMSE of the AOA estimation. The phase differences of the array signal are lost when we reconstruct the original signal. So, we can not get the AOA estimation from the reconstructed signal. Furthermore, we also can not get the array signal model by using RD sub-Nyquist sampling structure which is an one-branch structure.

Fig. 8 shows the spatial spectrum of the corrected compressed sampling data with the proposed method and the spatial spectrum of the uncorrected compressed sampling data with SNR $= 15$ dB. It can be seen from Fig. 8 that we can get the AOA estimation of the incident signal correctly by processing the corrected compressed sampling data. Moreover, we can not get the true spatial spectrum of the incident signal by directly processing the uncorrected compressed sampling data.

Fig. 9 shows the RMSE of the AOA estimation and Cramer-Rao bound [28] when SNR varies from -10 dB to 20 dB with 5 dB steps and the number of snapshots is $L_2 = 100$. It can be seen from Fig. 9 that the RMSE of the AOA estimation and Cramer-Rao bound decrease when SNR increases. Moreover, the RMSE of the AOA estimation is very close to Cramer-Rao bound when SNR ≥ -5 dB, which

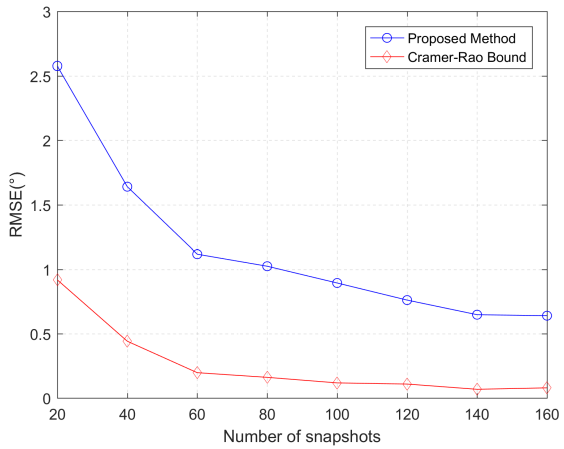

FIGURE 10. RMSE of AOA estimation versus number of snapshots.

declares that the proposed AOA estimation method by using the ULA based system can achieve a good AOA estimation performance.

Fig. 10 shows the RMSE of the AOA estimation and Cramer-Rao bound in the case of the number of snapshots varying from 20 to 160 in steps of 20 and SNR = 0 dB. It can be seen from Fig. 10 that the RMSE of the AOA estimation and Cramer-Rao bound decrease when the number of snapshots increases. In addition, the RMSE of the AOA estimation is more and more close to Cramer-Rao bound with the increase of the number of snapshots. It also validates the effectiveness of the proposed AOA estimation method by using the ULA based system.

V. CONCLUSION

In this paper, we propose a new MWC discrete compressed sampling structure based receiver which can be applied in the electronic reconnaissance and further propose a ULA based MWC discrete compressed sampling structure to estimate the carrier frequency and AOA simultaneously instead of the proposed receiver for the first time. The proposed receiver and ULA based system both have these advantages such as realizing sub-Nyquist sampling, solving the cross-channel signal problem flexibly, and having a low complexity of hardware implementation. In order to get the carrier frequency and AOA estimation with the ULA based system, we propose to use the cyclic-shifted pseudo-random sequences to mix the received signal. The ULA compressed sampling data are directly processed to get the estimation of the index of the sub-band where the original carrier frequency exists with the proposed method. Then, we can get the original carrier frequency estimation based on the estimations of the sub-band index and the baseband carrier frequency. Meanwhile, we can correct the phase differences of the ULA compressed sampling data based on the estimation of the sub-band index in order to estimate AOA with MUSIC algorithm. Finally, the simulation results of estimation performance and some discussions are shown. These analyses and trials illustrate the proposed system and method are effective and may be applied to practical applications. However, considering the joint carrier frequency and AOA estimations for the multi-signals in a large sampling time which is different with the assumption of this paper, we should know how to match the index of the sub-band with the corresponding signal, this may be a hard work. We will work on this aspect in the future.

REFERENCES

[1] K. George and C.-I. H. Chen, "Multiple signal detection digital wideband receiver using hardware accelerators," *IEEE Trans. Aerosp. Electron. Syst.*, vol. 49, no. 2, pp. 706–715, Apr. 2013.

[2] J.-D. Zhu, J.-L. Li, X.-D. Gao, L.-B. Ye, and H.-Y. Dai, "Adaptive threshold detection and estimation of linear frequency-modulated continuous-wave signals based on periodic fractional Fourier transform," *Circuits, Syst., Signal Process.*, vol. 35, no. 7, pp. 2502–2517, Sep. 2016.

[3] W. Yi, Z. Chen, R. Hoseinnezhad, and R. S. Blum, "Joint estimation of location and signal parameters for an LFM emitter," *Signal Process.*, vol. 134, pp. 100–112, May 2017.

[4] A. Coluccia and G. Ricci, "ABORT-like detection strategies to combat possible deceptive ECM signals in a network of radars," *IEEE Trans. Signal Process.*, vol. 63, no. 11, pp. 2904–2914, Jun. 2015.

[5] B. Zhao, F. Zhou, and Z. Bao, "Deception jamming for squint SAR based on multiple receivers," *IEEE J. Sel. Topics Appl. Earth Observ. Remote Sens.*, vol. 8, no. 8, pp. 3988–3998, Aug. 2015.

[6] J. Wu, D. Yang, and Z. Chen, "Design and application of multi-stage reconfigurable signal processing flow on FPGA," *Comput. Elect. Eng.*, vol. 42, pp. 1–11, Feb. 2015.

[7] T. Chen, P. Li, W. Zhang, and Y. Liu, "A novel channelized FB architecture with narrow transition bandwidth based on CEM FRM," *Ann. Telecommun.*, vol. 71, nos. 1–2, pp. 27–33, Feb. 2016.

[8] L. Anitori, A. Maleki, M. Otten, R. G. Baraniuk, and P. Hoogeboom, "Design and analysis of compressed sensing radar detectors," *IEEE Trans. Signal Process*, vol. 61, no. 4, pp. 813–827, Feb. 2016.

[9] P. Stinco, M. S. Greco, and F. Gini, "Spectrum sensing and sharing for cognitive radars," *IET Radar, Sonar Navigat.*, vol. 10, no. 3, pp. 595–602, Feb. 2015.

[10] B. Fang, G. Huang, and J. Gao, "Sub-Nyquist sampling and reconstruction model of LFM signals based on blind compressed sensing in FRFT domain," *Circuits, Syst. Signal Process.*, vol. 34, no. 2, pp. 419–439, Feb. 2015.

[11] L. Xu, Y. Ren, S. Sun, and Z. Cao, "Compressive sensing-based wideband capacitance measurement with a fixed sampling rate lower than the highest exciting frequency," *Meas. Sci. Technol.*, vol. 27, no. 3, p. 035006, Mar. 2016.

[12] M. Mishali and Y. C. Eldar, "From theory to practice: Sub-Nyquist sampling of sparse wideband analog signals," *IEEE J. Sel. Topics Signal Process.*, vol. 4, no. 2, pp. 375–391, Apr. 2010.

[13] E. Yang, X. Yan, and K. Qin, "Modulated wideband converter with run length limited sequences," *IEICE Electron. Exp.*, vol. 13, no. 17, p. 20160670, Sep. 2016.

[14] Z. Xu, Z. Li, and J. Li, "Broadband cooperative spectrum sensing based on distributed modulated wideband converter," *Sensors*, vol. 16, no. 10, pp. 1602–1613, Oct. 2016.

[15] N. Yu, X.-H. Qi, and X.-L. Qiao, "Multi-channels wideband digital reconnaissance receiver based on compressed sensing," *IET Signal Process.*, vol. 7, no. 8, pp. 731–742, Oct. 2013.

[16] S. A. Abbas, Q. Sun, and H. Foroosh, "Frequency estimation of sinusoids from nonuniform samples," *Signal Process.*, vol. 129, pp. 67–81, Dec. 2016.

[17] F. G. Sun, B. Gao, L. Z. Chen, and P. Lan, "A low-complexity ESPRIT-based DOA estimation method for co-prime linear arrays," *Sensors.*, vol. 16, no. 9, pp. 1367–1375, Sep. 2016.

[18] K. Wang, J. He, T. Shu, and Z. Liu, "Localization of mixed completely and partially polarized signals with crossed-dipole sensor arrays," *Sensors.*, vol. 15, no. 12, pp. 31859–31868, Dec. 2015.

[19] T. Chen, L. Liu, and Z. Zhao, "A frequency estimation method based on MWC discrete compressed sampling structure," in *Proc. IEEE 6th Int. Conf. Instrum. Meas. Comput. Commun. Control*, Harbin, China, Jul. 2016, pp. 274–278.

[20] O. Yair, S. Stein, D. Cohen, and Y. C. Eldar, "Uniform linear array based spectrum sensing from sub-Nyquist samples," in *Proc. IEEE Global Commun. Conf.*, San Diego, CA, USA, Dec. 2015, pp. 1–6.
[21] S. Stein, O. Yair, D. Cohen, and Y. C. Eldar, "Joint spectrum sensing and direction of arrival recovery from sub-Nyquist samples," in *Proc. IEEE 16th Int. Workshop Signal Process. Adv. Wireless Commun.*, Stockholm, Sweden, Jun./Jul. 2015, pp. 331–335.
[22] C.-H. Cheng, "Wideband receiver with I/Q channels for multiple Nyquist zone coverage," *IET Radar, Sonar Navigat.*, vol. 9, no. 4, pp. 421–428, Apr. 2015.
[23] T. Chen, H. Wu, and Z. Zhao, "The real-valued sparse direction of arrival (DOA) estimation based on the Khatri–Rao product," *Sensors*, vol. 16, no. 5, pp. 693–705, May 2016.
[24] C.-Y. Chen, W.-R. Wu, and C.-S. Gau, "Joint AoA and channel estimation for SIMO-OFDM systems: A compressive-sensing approach," *J. Signal Process. Syst.*, vol. 83, no. 2, pp. 191–205, May 2016.
[25] X. Wang, Y. Xiong, and W. Huang, "An accurate direction finding scheme using virtual antenna array via smartphones," *Sensors*, vol. 16, no. 11, pp. 1811–1832, Nov. 2016.
[26] A. Chaturvedi and H. H. Fan, "Wideband delay and direction of arrival estimation using sub-Nyquist sampling," *Signal Process.*, vol. 135, pp. 67–80, Jun. 2017.
[27] L. Liu and H. Liu, "Joint estimation of DOA and TDOA of multiple reflections in mobile communications," *IEEE Access*, vol. 4, pp. 3815–3823, Jun. 2016.
[28] Q. Wang, H. Yang, H. Chen, Y. Dong, and L. H. Wang, "A low-complexity method for two-dimensional direction-of-arrival estimation using an L-shaped array," *Sensors*, vol. 17, no. 1, pp. 190–203, Jan. 2017.

TAO CHEN received the B.S. degree in information engineering, the M.S. degree in signal and information processing, and the Ph.D. degree in communication and information systems from Harbin Engineering University, Harbin, China, in 1997, 2001, and 2004, respectively.

He is currently a Professor with the College of Information and Communication Engineering, Harbin Engineering University. His research interests include wideband signal detection, processing, and recognition.

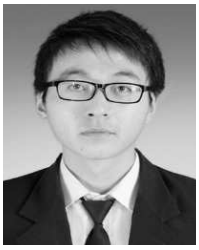

LIZHI LIU received the B.S. degree in electronic and information engineering from the Harbin Institute of Technology, Weihai, China, in 2015. He is currently pursuing the M.S. degree with the College of Information and Communication Engineering, Harbin Engineering University, Harbin, China.

His research interests include wideband signal detection, processing, and recognition.

DAPENG PAN received the B.S. degree and the M.S. degree in information and communication engineering from Harbin Engineering University, Harbin, China, in 2002 and 2007, respectively, where he is currently pursuing the Ph.D. degree with the College of Information and Communication Engineering, Harbin Engineering University.

He is currently a Lecturer with the College of Information and Communication Engineering, Harbin Engineering University. His research interests include wideband signal detection, processing, and recognition.